PROJECT FINAL REPORT

Grant Agreement number: 252935

Project acronym: Assay for Biomarkers

Project title: Magnetic Nanoparticles for multiplexed assays for low and high molecular weight biomarkers.

Funding Scheme:

Period covered: **from** June 09 **to** March 2010

Prof Gil U. Lee. Stokes Professor
Bionanoscience Group
University College Dublin School of Chemistry, Belfield. Dublin D4
Tel: 01 716-2399

Fax:

E-mail: gil.lee@ucd.ie

Project website http://bionano.ucd.ie/ **address:** Bionanoscience group. Centre for Nanomedicine, School of chemistry and chemical biology. Science Building South, University college Dublin. Belfield.
Dublin 4.

Executive Summary

The application for the FP7-PEOPLE-2009-IEF was to support a move of a postdoctoral researcher to University College Dublin, UCD. The researcher as the time of moving had published 16 peer reviewed journals with a h-index of 8. With the expert training and opportunities in place at UCD, the award of the fellowship hoped to build upon the successful start to his academic career and deliver him to a full time academic position. Upon completion of the proposal the fellow leaves with 22 publications, with cover 240 citations and has seen his h-index increase to 9. The fellow has been involved with three patent applications, and leaves the project to join the Chemistry department at the University of Loughborough taking up a lectureship position.

The research proposal outlined a technique for the detection of biomarkers with the capability of working directly in biological samples. The technique aimed to deliver nanoparticles that contained paramagnetic and optical properties, which could be functionalized with aptamers/ or antibodies. These functionalized particles would capture the biomarkers directly from solution, and in conjunction with an in-house technology named non-linear magnetophoretic separation, NLM, would allow the quick separation and detection by exploiting the particles superparamagnetic and optical properties, creating a new diagnostic technology. In developing the researchg it was apparent that the in-house NLM technology was not suitable for the detection of the analytes at this time and required further development. The fellow has contributed to the enhancement of the technology yielding publication in preparation. To circumvent the need of a detection platform a second technology was identified. A new emerging technology of tunable nanopore was utilised and has delivered a patent application, publications and commercial interest. Whilst the technology platform has changed from the initial proposal the ultimate aim has been secured.

The ultimate deliverable was a process capable of capturing the analyte as well as performing the initial sample purification and pre-concentration stage that screens multiple biomarkers for several diseases across a wide range of molecular weights and functionalities. Delivering the benefits of being both a multiplexed technique with the highly desirable tagless detection mechanism. The fellow has researched the key parameters for such assays as well as a new technology for ths assay using nanopore technology. It has been demonstrated with aptamer capture probes and biomarker targets. The work has been showcased at two international conferences and has been the subject of commercial interest.

The training that accompanied this proposal aimed to ensure the fellow received a broad scientific understanding, crossing several scientific fields delivering an interdisciplinary research approach. When combined with the support infrastructure at UCD, it has delivered outstanding career enhancement prospects to the applicant, delivering a new diagnostic technique to enhance the European research portfolio. The applicant has been a mentor to two PhD students and has participated in teaching chemistry to undergraduate students.

Summary description of project context and objectives

Introduction.

We deliver a new powerful diagnostic technique, built upon advances in the fields of separation and nanoparticle technologies. The scope of this technique and its far reaching implications will be demonstrated by the detection of large proteins and peptides alongside the detection of a small organic molecule. This allows the simultaneous detection of biomarkers covering multiple omic fields of research. The range of analytes that this technique is capable of detecting is made possible by developing new aptamer tagless detection strategies which will be incorporated for the first time onto nanoparticles. This approach will set the technique aside and beyond existing methods by combining several experimental aspects into one process. It has the capability to capture of the analyte, as well as perform sample preparation and extraction using magnetic particles, coupled with a fast and sensitive detection mechanism using both flow cytometry and nanopore technologies. This makes the outlined technique both simpler than existing alternative techniques such as mass spectroscopy or array based technologies, but it also produces a low tech miniaturized diagnostic device that has the capacity to be used in developing countries.

Microarrays are the dominant format for screening larger numbers of targets simultaneously, and are capable of yielding huge quantities of data at both the genomic and the proteomic level. Whilst there currently exist several commercially available antibody arrays, capable of screening for cell pathways or signalling sets, an equivalent format capable of screening metabolites is currently sought. Aptamers offer an alternative technology to antibodies, and since they were first raised in the 1990s, researchers have been quick to exploit their potential, with applications in drug candidate validation, therapeutics and diagnostics. An array combining both antibodies and aptamers would allow the screening of a large range of biomarkers spanning a range of molecular weights and functionalities. A limiting factor in creating such an array lies in the fact detection methods typically rely upon the analytes to be labelled/ tagged using either a dye, enzyme or redox centre. Apart from introducing an additional experimental step and costs, it can be tedious and difficult to do for high throughput applications. In addition to this the label itself can often alter the method and strength of the biomolecular interaction leading to false positive of reduced sensitivity.

Metallic rods with nanoscale dimensions have been shown to be ideal reporters, sensors and diagnostic delivery agents. Our outlined fabrication process generates large quantities of particles with uniform and desirable characteristics. Huge efforts are underway to provide tagless detection mechanisms in diagnostic devices. Our proposed studies, provide a new route for tagless detection, highly publishable in itself, but would also provide a much sought after multiplexed assay.

We demonstrate this technology using technique with a variety of biomarkers with known antibodies and aptamers, once proven this technique will be quickly and easily adaptable to multiple systems as researchers discover new biomarkers for a range of diseases. With the use of aptamers along side this technology and their growing body of research demonstrating the ease of modification and development of sequences. It is evident that if a tagless detection platform can be created, aptamer technologies can deliver a means to capture a diverse range of analytes.

Initially we use spherical beads and the flow cytometry technology to probe the kinetics and key parameters for particle aggregation and define the key parameters for tagless detection. We conclude with a new nanopore technology using multicomponent nanorods.

Technology One – Flow cytometry and the detection of sexually transmitted infections

The miniaturization of laboratory instrumentation through microfabrication and the development of novel nanomaterials have produced powerful new technologies that promise to expand the application of POC diagnostics and prognosis. POCT can now be applied to a range of diseases but some of these technologies are limited by turnaround time, specificity, sensitivity, and cost. For example, when screening for sexually transmitted infections, STIs, rapid diagnosis is critical as delays can lead to progression to chronic disease, infertility, cancer, and contribute to continued pathogen and disease transmission. However, STIs are often present in samples at levels below the sensitivity of POCT and analysis typically takes longer than is acceptable for a POC visit.

Flow cytometry is a powerful analytical technology that has recently undergone a significant decrease in cost and size due to advances in solid-state optics and microfluidics. FC has the ability to be miniaturized to small bench top systems, offers continuous throughput of samples and multiplexing of analytes. FC can be easily modified in research laboratories using a range of fluorescent probes and nanoparticles, e.g., the use of quantum dots for the detection of multiple biomarkers.

POCT often requires pretreatment involving purification or filtration. *SPMs* provide an efficient and cost effective way to separate and pre-concentrate analytes from solutions helping to simplify and facilitate the front-end of an assay. They are readily available through numerous commercial sources and synthesis strategies, offering a range of surface chemistries that can be quickly conjugated to any capture probe of interest. SPMs have demonstrated their versatility for use in conjunction with techniques such as the polymerase chain reaction, mass spectroscopy and have been utilized in high-throughput linear magnetophoresis, LM, assays. Detection of the analyte in LM can be performed by characterizing the physical properties of the magnetic beads in the presence of the target producing a "label-free" detection platform. If the target analyte contains multiple epitopes, then it is possible for the target to bind to multiple beads simultaneously, leading to aggregation, shown schematically in Figure A1. This aggregation has been utilized in LM, allowing the detection of the dengue virus at 10 plaque forming units/ml. Alternative methods have relied upon two main modes of detection. The first monitors the aggregation as a function of analyte concentration measuring chain length or turbidity whereas the second monitors the change in magnetic properties as particles are forced to be in close proximity to each other. These techniques have detection levels down to picomolar levels, with assay times as low as 5 minutes, but have a limited dynamic range and promise to be difficult to multiplex.

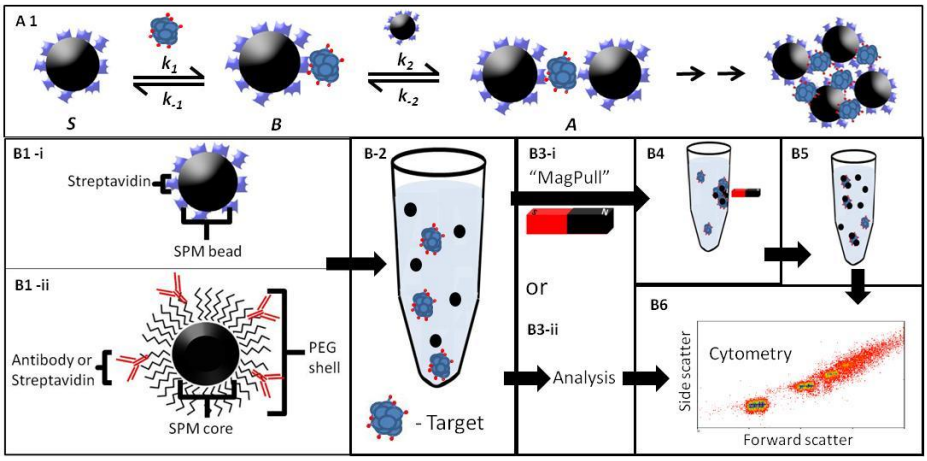

Figure 1. *Schematic of MBA-FC assay based.* ***A*** *Capture of analyte and aggregation of SPMs using MBA.* ***B1*** *SPM's were either (i) purchased with a streptavidin monolayer or (ii) carboxyl beads were coated with PEG and conjugated to an antibody of choice.* ***B2*** *SPM's were incubated with target.* ***B3i*** *Aggregation of the beads was aided by the use of a*

magnetic field. ***B3-ii*** *Samples can also be analysed without MBA.* ***B4/B5*** *Using the magpull strategy the beads may be washed and resuspended before analysis.* ***B6*** *The aggreation state of the SPMs was determined using flow cytometry.*

In this section we examine the key physical and chemical parameters influencing a MBA assay that is illustrated in Figure 1. FC was used as it provides a means to fully characterize the agglutination state of all magnetic particles in the sample and is a piece of equipment that is commonly found in infectious disease reference laboratories. We first identified the key parameters that control the aggregation of SPMs for the streptavidin-biotin assay, i.e., bead concentration, binding capacity, reaction time, and application of magnetic force. The streptavidin-biotin interaction was used as a model as it is among the strongest known noncovalent specific molecular interactions, i.e., $K_d \sim 10^{-15}$ M. Under the optimal assay conditions the MBA-FC assay could be used to detect biotin across six orders of magnitude in concentration with sensitivities in the fM level. We then demonstrated the applicability of the MBA-FC assay for the detection of the HSV-1 and 2 viruses. The antibody-based assay highlighted the role of binding target and affinity in the sensitivity of the MBA. We demonstrate here that by utilizing their magnetic properties in the presence of a magnetic field, the speed, and sensitivity of an MBA assay can be increased**.**

Technology two – Nanopore technology and the detection cancer reporters

The characterization of colloid and nanoparticle based systems has been aided in recent years by the resurgence and development of Coulter counting and micro- to nanopore based technologies. Collectively known as resistive pulse sensing (*RPS*) they offer an attractive technology format because the measurements provide information on individual particles within their natural environment. RPS has been used to study numerous types of particles, including single molecules, proteins, biological and synthetic nanoparticles. Pores typically fall into two categories, biological or solid state. Biological nanopores such as α-haemolysin, which has a diameter of 1.4 nm at its narrowest point, have been used to detect and observe ssDNA. Whilst biological pores offer an insight into single molecules and cellular mechanisms, their fixed size, stability and compatibility in systems with variable pH, ionic strength and temperatures can limit their applications. Solid-state nanopores often support more chemical versatility, but have fixed pore diameters, with carbon nanotubes, PDMS, glass, silicon and polycarbonate having been used as substrates.

Recently, tunable elastomeric pore technologies have emerged, allowing further versatility as the pore can be stretched in real time to suit the sample. Tunable pores (*TP*s) are fabricated by mechanically puncturing a thermoplastic polyurethane membrane. The membrane can be stretched in a controlled, reversible fashion to change the pore geometry – altering the size of the pore by as much as an order of magnitude. Techniques have been developed for using TPs to accurately determine the concentration, size and surface charge of dispersed inorganic particles. Capable of detecting biological particles as well as discriminating between particles of different functionalization, TPs are typically used to measure particles with one dimension larger than 100 nm. Detailed studies of resistive pulse shapes could allow studies of particle morphology, and aggregation of 1 μm superparamagnetic spheres has recently been investigated using TPs.

In RPS experiments, the TP is filled with a conducting medium, and a potential is applied between two electrodes on either side of the pore opening. This establishes a current flow through the pore, known as a base line current (i_p), which is usually proportional to the applied voltage and electrolyte conductivity. Previous work has discussed analytical and semi-analytical descriptions of the baseline current in TPs, and the current change caused when a particle moves through a pore (Δi_p, Figure 2). For a simple cylindrical pore, the latter is given by,

$$\frac{\Delta i_p}{i_p} = \frac{S(d_p, d_s)(d_s^3)}{(l_p + 0.8 d_p) d_p^2} \qquad (1)$$

where l_p is the pore length, d_p is the pore diameter, d_s is the diameter of a spherical particle, and $S(d_p,d_s)$ is a correction factor that depends on d_p and d_s. Although TPs are conical, the

proportionality between Δi_p and particle volume in Equation (1) still holds to a good degree of accuracy, and can be used for particle sizing. The change in current is one of two measurements used for this study, the second being the full width half maximum (FWHM) duration of the resistive pulse, which indicates the time taken for the particle to traverse the pore. The velocity of the particle is generally determined by contributions from pressure driven flow, electrophoresis, electro-osmosis and diffusion. In the present work, flow caused by an inherent pressure head ($P_1 > P_2$ in Figure 2a) dominates the other mechanisms.

Nanoparticles with magnetic properties are increasingly being used in diagnostic assays, either to aid sample purification or to facilitate detection. Again we use the simple detection strategy utilizes an analyte's capacity to simultaneously bind to multiple particles, leading to aggregation. Particles are typically synthesized with dual functionality i.e. an optical property for detection and a magnetic component to aid separation, and particle synthesis routes are numerous, from Janus-particles to core shell configurations. Electrodeposition within a template offers an alternative route to producing particles, as the particles can be synthesized to contain several materials, giving the appearance of a barcode. Rod shaped particles offer an intriguing advantage over spheres in agglutination assays, as rods have two physical dimensions which can be changed, diameter and length. Rods of varying aspect ratios can be assigned to capture an analyte, and the frequency of their aggregates counted. Additionally, rods have been shown to aggregate in different configurations: end-to-end, or forming rafts.

We present the first measurements of rod shaped synthetic particles using a TP, and demonstrate that a clear and reproducible signal can be observed. We characterized and modelled the signal from the particles as they traverse the pore and relate Δi_p to the size of the particle. The data suggest that the FWHM is related to the rod length, and indicate that the particles traverse the pore in various orientations. Utilizing both measurements, an new agglutination assay was designed and demonstrated using two capture probes, the model biotin-avidin system and a DNA aptamer system. Aptamers are oligonucleotide or peptide sequences that are capable of binding to targets with high specificity and selectivity. Their low production costs and the range of analytes to which they can bind make them an attractive alternative to antibodies. The aptamer chosen here is the 35mer sequence which binds to the protein platelet derived growth factor, PDGF-BB, with a $K_d \sim 0.1$ nM. The ability to detect PDGF is of interest as it is one of numerous growth factors over expresed in the serum of cancer patients, particularly those with lung and pleural tumors. Here the aggregation of rods is used to detect the PDGF protein down to fM levels of sensitivity with an assay time on the order of 10 minutes.

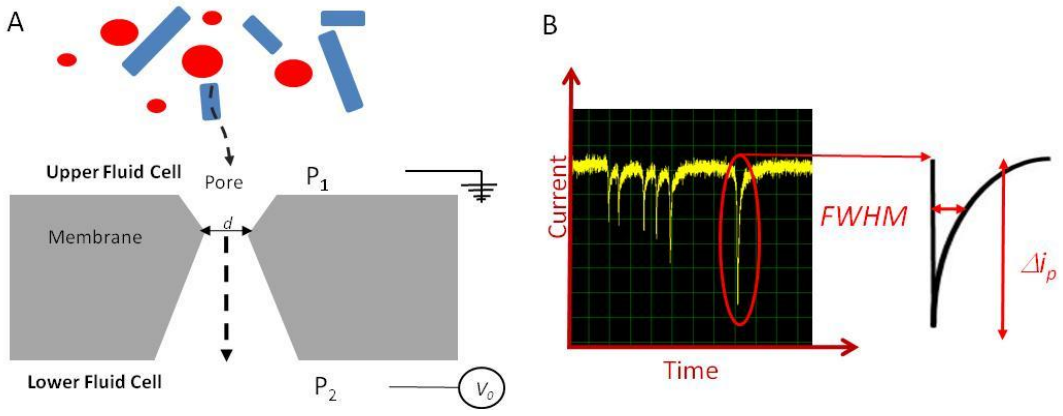

Figure 2. Overview of resistive pulse sensing with tunable pores. A – Sectional schematic of a pore. The sample is placed into the upper fluid cell. B – Example of baseline current and "blockade" events (dips in current) that are each caused by a particle passing through the pore. Each event is analysed for full width half maximum (FWHM) duration and Δi_p.

- A description of the main S&T results/foregrounds (not exceeding 25 pages),

Results technology One – Flow cytometry and the detection of sexually transmitted infections

Detection of biotinylated BSA with MBA-FC

Figure 1 illustrates the three steps that were used to execute the MBA-FC assay for the model BBSA-streptavidin (SA) system. In the first step, shown in Figure 1B2, streptavidin functionalized SPMs were reacted with BBSA that have an average of 9 biotin molecules per BSA protein. The SPM's for MBA-FC need to be highly uniform in diameter as this makes the FC signal from the aggregates easy to identify. In this study, commercial Dynal beads were used as they have a relatively uniform size, i.e., <2% *coefficient of variation, CV*[33], and a number of particle sizes are available, i.e., 1 and 3 μm. In the second step, shown in Figures B3 to B5, a magnetic gradient was applied to the bead suspensions to separate the beads and accelerate the rate of bead interaction with each other. In the final step, shown in Figure B6, the SPM aggregation state was determined by FC. The magnetic separation procedure, steps B-3 to B-5, took approximately 3 minutes to complete and the FC analysis could be completed in approximately 5 minutes.

Figure 3A presents the FC analysis of 100,000 particles for MBA assays over six orders of magnitude of BBSA concentration for 3 μm streptavidin functionalized beads. The *x*-axis of these figures presents forward scatter intensity, which is characteristic of bead size, and the *y*-axis presents side scatter intensity at 488 and 635 nm. The fluorescence in the side-scatter signal was produced by the auto-fluorescence of the SPMs. The fluorescence signal was not required to complete these measurement but fluorescent markers could easily be employed to aid the analysis in the case in which multiple analytes are being simultaneously measured. It is clear from this figure that the FC signals shift towards higher foreword and side scattering in the presence of BBSA, which is a characteristic of bead aggregation. Three other trends can be observed in these results. First, the presence of a large cluster of data points that represents the individual beads, or monomers, was present in the bottom, left corner of all plots. This feature is confirmed when a sample of beads without the addition of an analyte is passed through the FC (data not shown). Second, the narrow size distribution of the SPMs resulted in tightly packed clusters of data points making the numbers of specific aggregates relatively easy to identify as defined by the boxes delineated by dashed lines in Figure 3A. Third, all cluster populations were observed to increase as the concentration of BBSA was increased from $3x10^{-14}$ to 3 nM. However, at 300 nM BBSA the number of clusters was observed to decrease.

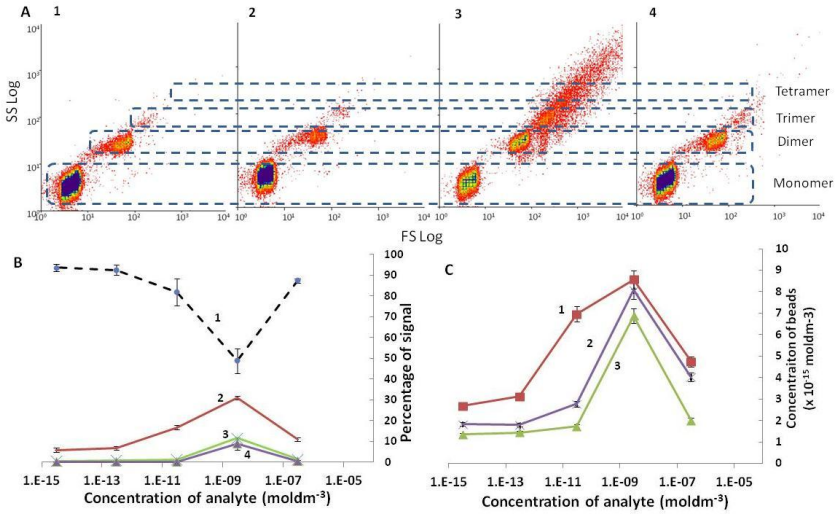

Figure 3. *Influence of magnetic field and reaction time on the response of the biotin-streptavidin MBA-FC assay (all assays undergo magpull unless specifically stated).* ***A*** *FC analysis of assays executed using 50 fM of 3 μm streptavidin beads with a binding capacity 75 nM, 30 min reaction time. BBSA at concentrations of 1) 3 x 10^{-4} nM, 2) 0.03 nM, 3) 3 nM, and 4) 300 nM.* ***B*** *Distribution of monomers (1), dimers (2), trimers (3), and tetramers (4) for the reaction conditions described above.* ***C*** *Concentration of dimers in MBA as a function of analyte concentration for a 30 min reaction with MBA (1), 5 min reaction with MBA (2), and 5 min reaction without magnetic field (3). Blank assays were found to have aggregatoin levels below 3±2% in all assays in this study.*

Figure 3B summarizes the quantitative analysis of the percentage of monomers, dimers, trimers and tetramers formed in the MBA assay as a function of BBSA concentration over ten orders of magnitude. Conservation of the total number of SPMs meant that the formation of aggregates was closely correlated with the decrease in monomers, i.e., the minimum number of monomers appeared at a BBSA concentration at which the maximum number of dimers, trimers, and tetramers were observed. At concentrations between 10^{-15} and 10^{-9} M there was a direct correlation between the number of dimer aggregates and the biotin-BSA concentration. However, at concentrations of BBSA greater than 1 nM there was a sharp decrease in number of all forms of aggregates and increase in monomers was observed. The decrease in signal from aggregation at high concentrations of analytes has been well document for agglutination assays. It results from the saturation of the particle surface with analyte and is known as the 'hook' effect. It is also clear that a significant numbers of trimer and tetramer aggregates form at 10^{-8} M BBSA, which appears to be characteristic of the higher coverage of biotin on the beads.

Influence of reaction time and magnetic force on the MBA assay sensitivity

Figure 3C presents the number of dimers formed as a function of BBSA concentration, reaction time, and magnetic field. Several observations can be made from these results. First, increasing the reaction time from 5 to 30 minutes resulted in a significant increase in the fraction of dimers formed in the MBA assay in the concentration range between 10^{-13} and 10^{-9} M. The 30 minute assay results presented in curve 1 demonstrate sensitivities as low as 10^{-13} M while the lowest concentration signal that can be observed in the 5 minute assay in curve 2 was 10^{-11} M. Second, application of magnetic force to the SPMs resulted in an increase in the number of aggregates formed across the range of concentrations studied by approximately 1%.

The relevant time scale for the formation of aggregates was a result of at least three factors, i.e., the rate of the reaction of BBSA with the streptavidin on the beads, the convective mass transport to the BBSA to the SPMs, and the reaction of the SPMs with each other to form aggregates. Previous studies have revealed that the rate of protein reactions are much faster than the rate of diffusion of proteins in water, i.e., the second Damkohler number is significantly greater than 1[12]. Thus, the convective transport of BBSA to the microparticles was the rate-limiting step that determined the coverage biotin on the SPMs. The relevant time constant for convection mass transport is $t = \frac{\langle x \rangle}{h}$, where $\langle x \rangle$ is the average distance between particles and h is the convection coefficient of the SPM. The average convection coefficient for a sphere in the limit of the low Reynolds number flow, that takes place in these reactions, is simply $h = \frac{D}{r_h}$, where D is the diffusion coefficient and r_h is the hydrodynamic radius. The diffusion and convection coefficients of a 3 μm diameter bead are 1.5×10^{-8} cm^2/s and 2.9×10^{-6} cm/s, respectively. Thus, the time scale for the BBSA transport to the microparticle was 600 seconds for a particle density of 6.25×10^7 per milliliter, which is equivalent to 50 fM of beads. Thus, the relevant time scale for the reaction was 10 minutes. The increase in the sensitivity of the assay for the 30 minute reaction time can thus be linked to the convective transport of BBSA. The convective time constant can be decreased by increasing the

convention coefficient or decreasing the characteristic length scale. This can be achieved by using smaller particles or higher densities of particles, respectively.

In previous studies the relationship between the bead aggregation and analyte concentration has been defined as the efficiency[28]. A 100% efficiency arises from a 1:1 relationship between dimers and target analyte, i.e., a reaction with 100% efficiency would produce 50 dimers in a sample of 50 analytes per ml. Efficiencies as high as 70% have been achieved for beads with diameters between 20 and 200nm[28]. In this study, 50 fM of 3 μm diameter SPMs were used that had a total streptavidin concentration of 75 nM. The MBA BBSA reaction efficiency was significantly less than 1%. These relatively low reaction efficiencies appear to be a characteristic of the larger beads used in this study. The rotational diffusion coefficient scales as $[r_h]^{-2}$ and thus 3 μm bead spontaneously rotate at a rate 225 times slower that a 200 nm bead. The larger beads will thus have a higher steric factor to overcome for the alignment of the capture probe and target. The complexity of the interaction, will also an important factor. Here biotin projects from the protein on a linker and is capable of free rotation around a single bond, and thus should be able to orientate itself with a neighboring streptavidin protein relatively easily.

The influence of magnetic forces on the assay was determined by analyzing aggregate formation with and without magnet field. Curves 2 and 3 in Figure 3C, have a similar form at high concentrations of analyte the curves, but at lower analyte concentrations the number of measured aggregates in the presence of the magpull was always greater, demonstrating the enhancement of the aggregation. It was striking, however, that there a relatively low efficiency for dimer formation still exists, which suggests that the reaction of the biotin immobilized on the 3 μm SPMs was not very efficient. The low efficiency of the assay clearly limits the sensitivity of the assay but also means that MBA assay provides a signal over six orders of magnitude.

Influence of bead size and binding capacity and size on the response of MBA

To further investigate the sensitivity, dynamic range, and hook effect of the MBA assay, a set of experiments were devised in which the binding capacity and bead concentration were systemically varied. Figure 4A presents the percent of dimers produced by the reaction of 3 μm SPMs with BBSA at concentrations ranging between 10^{-14} and 10^{-6} M for 30 min. Curves 1 and 2 present the results for a SPM bead concentration of 50 fM with streptavidin coverages of $2x10^6$ and $2x10^5$ molecules per bead, respectively. Curve 3 presents the results for a SPM bead concentration of 5 fM and streptavidin coverage of $2x10^6$ molecules per bead. Three observations can be made about these results. First, decreasing the concentration of streptavidin density on the beads resulted in a significant decrease in the fraction of dimers formed at a given BBSA concentration. This resulted in a corresponding decrease in sensitivity for the lower coverage beads. Second, decreasing the number of beads at the higher streptavidin coverage resulted in a higher sensitivity of the assay but also an earlier on-set of the hook effect. Third, decreasing the number of beads did not decrease the sensitivity of the assay, which confirms that the rate of convective transport of BBSA to the beads is not the rate limiting step in the formation of dimmers.

The onset of the hook effect was found to be closely linked to both the concentration of streptavidin in the reaction and the density of streptavidin on the beads in the reactions in Figure 3A. In each reaction the maximum number of dimers formed at a BBSA concentration just under the streptavidin concentration on the beads. This was to be expected, as the maximum number of dimmers should occur just before the BBSA saturates the streptavidin sites on the beads. However, the exact ratio at which the BBSA saturates streptavidin appears to be dependent on the density of streptavidin on the beads. For the high streptavidin coverage, which was close to a monolayer, the BBSA appears to start to saturate the streptavidin when it exceeds 10% of the streptavidin concentration. At submonolayer coverages of streptavidin, however, it appears the BBSA has to almost equal the streptavidin concenration before the surface is saturated.

To test the effect of particle size a similar set of experiments were then performed with BBSA for streptavidin functionalized 1 μm beads and the results are shown in Figure 4B. Qualitatively similar trends were observed, i.e., both the intensity and position of the maximum number of aggregates can be tailored by changing the bead number and binding capacity. Quantitatively, however, the results for the 1 μm beads differed from the 3 μm beads. It is clear from curve 2 in Figures 4A and B that the peak in aggregate concentration appeared at much lower concentration for a similar concentration of streptavidin and that a much larger of fraction of beads formed aggregates. The interpretation of this result is that when the same number of 1 and 3 μm beads are used the 1 μm beads aggregate more efficiently. This could result from the fact that the 1 μm beads have a higher density of streptavidin or that their rotational difficult coefficient her higher. The reaction of the 1 μm beads, however, still is not highly efficient (1.4%).

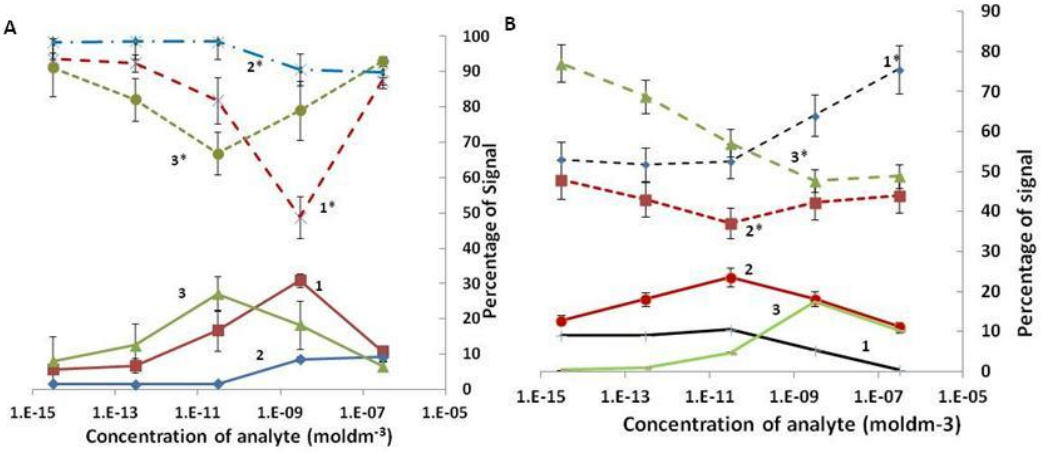

Figure 4*. Influence of bead properties on the response of the biotin-streptavidin MBA-FC assay.* ***A*** *Distribution of 3 μm bead monomers (denoted with *) and dimers as the bead concentration and binding capacity are varied. Curves 1 and 1* - 50 fM bead concentration, 75 nM binding capacity. Curves 2 and 2* - 50 fM bead concentration, binding capacity of 8 nM. Curves 3 and 3* - 5 fM bead concentration, binding capacity of 7 nM.* ***B*** *Formation of 1 μm bead monomers (denoted *)* ***)*** *and tetramers as the bead concentration and binding capacity of the beads are varied. Curve 1 and 1* - 5 fM bead concentration, binding capacity 0.52 nM. Curves 2 and 2* - 50 fM bead concentration, binding capacity 5.2 nM. Curves 3 and 3*- 500 fM bead concentration, binding capacity 52 nM These reactions were carried out in PBST buffer for 30 mins followed by magpull and FC analysis. Blank assays were found to have a aggregatoin levels below 3±2% in all assays in this study.*

Detection of HSV-1 and 2 with MBA-FC

We have demonstrated the clinical applicability of this technique by detecting HSV types 1 and 2 virus. Initially a polyclonal antibody was evaluated for the HSV-2 capture experiment, however, increases in particle aggregation in the presence of the analyte, were not observed. After switching to commercially available monoclonal antibodies a clearer signal was created, but only in the presence of magnetic field, again demonstrating the benefit of using SPM's in conjunction with the MBA. Binding constants for the HSV-1 monoclonal and polyclonal antibodies were measured via SPR. The on-rate between the antibodies are very similar, the off-rate however for the polyclonal was ~5 times faster. This may have resulted in the aggregates separating in the ~2 minutes from performing the MBA to running the sample in the FC for the polyclonal system; as such we used monoclonal antibodies throughout the remaining experiments.

A typical response from the 3 μm beads for the detection of HSV-2 is shown in Figures 5A. As the target antigen concentration increased the number of monomers decreased and the number of dimers, trimers and tetramers increased. Three observations can be made about the antibody results. First, a hook effect was not clearly observed in the results. This is attributed to the fact the antibodies were immobilized on the SPMs at a much lower concentration that the streptavidin

functionalized particles and that there are increased steric barriers associated with the binding of a large viral antigen with covalently immobilized antibody. Second, the monomer binding response was very broad taking place across six order of magnitude in virus concentration from 10^{-12} to 10^{-6} M. This response may be partially attributed to the low density of antibody but is also a result of the fact that antigen has multiple epitopes to which the antibodies can bind. This necessarily results in an increase in the observed avidity of the interaction and observed sensitivity of the assay well below the equilibrium constant of the antibodies, i.e., Kd = 10^{-8} M. Finally, the size of the particles, antibody and epitope had very little influence on the MBA assay response or sensitivity. Cleary, the behavior of the antibody assay highlights another key parameter that must be considered when designing aggregation assays, namely the affinity of the capture antibody and target.

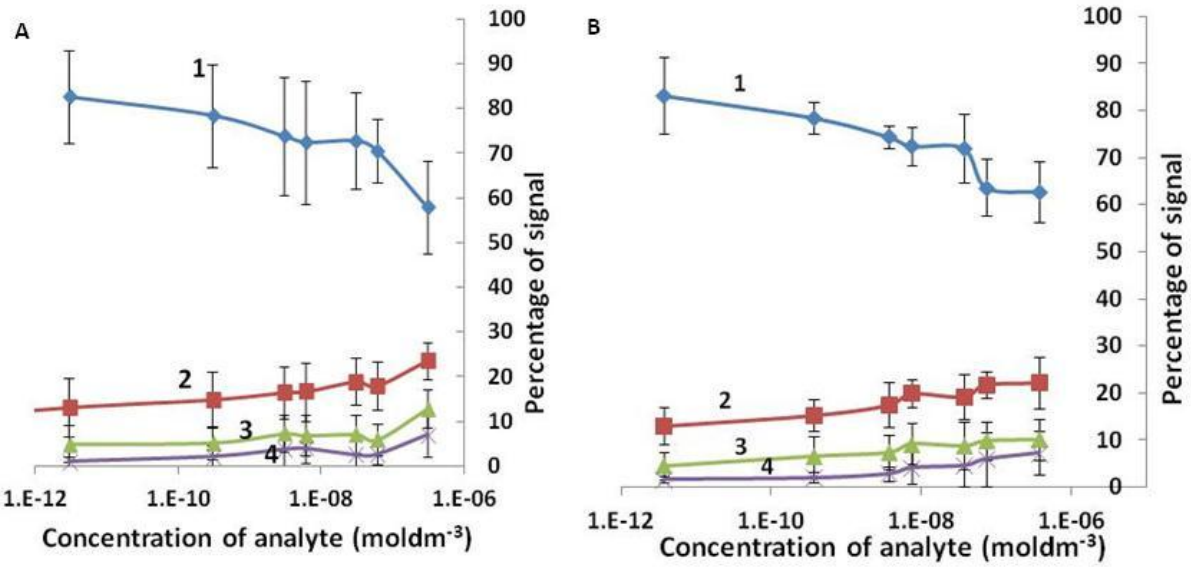

Figure 5. *HSV-1 and 2 MBA-FC assay - Curve 1 – monomers, 2 – dimers, 3 – trimers and 4 – tetramers of SPMs.* ***A*** *Formation of aggregates of 3 μm SPMs as a function of HSV-2 antigen concentration in PBST, 50 fM bead concentration, binding capacity of 3 nM.* ***B*** *Formation of aggregates of 1 μm SPMs as a function of HSV-1 antigen concentration in PBST, 500 fM bead concentration, binding capacity of 3 nM. In each assay the SPMs were reacted with the analytes for 30 mins in PBST. Blank assays were found to have a aggregation level below 3±2%.*

We initially investigated the key experimental variables in designing a magnetic aggregation assay and demonstrated its applicability using readily available commercial chemicals on a widely used diagnostic platform. A summary of all the factors that were found to influence the sensitivity of the assay is shown in Figure 6. It was clear from this analysis that the bead-bead reaction was the rate-limiting factor determining the number of aggregates formed and thus the sensitivity and response-time of the assay. This is somewhat surprising as the particles are forced into direct contact by the MBA assay and thus one would predict that the rates of reaction would be accelerated. However, this is consistent with previous studies of micron size SPM reacting with planar surfaces. In these single molecules measurements of the protein A-IgG interaction single molecule bonds were only observed to form after approximately 100 potential protein A-IgG interactions were allowed to interact with each other for 10's of seconds.

The resulting assay platform was capable of operating over six orders of magnitude of concentration with assay times as low as 5 minutes with sensitivities on the fM scale. The sensitivity of the assay could be increased by increasing the density of receptors on the beads, decreasing the size of the beads used, and decreasing the total number of beads used in the assay. However, higher sensitivities sometimes resulted in a more rapid the saturation of the beads with analyte and thus earlier onset of the hook effect. Thus, by controlling the particle size, binding capacity,

avidity/affinity, and particle concentration, the aggregation of SPM's in the presence of the target analyte can be tailored and predicted producing a simple and sensitive analytical method.

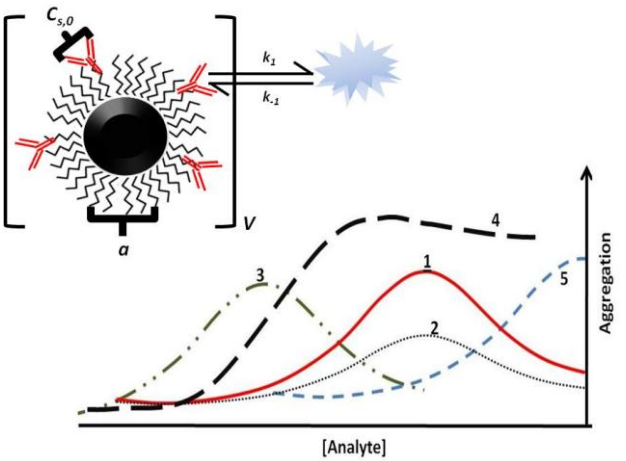

Figure 6. *MBA aggregation key parametres resulting from change in the physical and chemical properties of the SPMs. 1 - Reference bead area (a), volume (V), binding capacity ($C_{s,0}$), rate of reaction (k_1). 2 - Decrease $C_{s,0}$, constant a, V and k_1. 3 – Decrease a, increase V, constant $C_{s,0}$ and k_1. 4 – Decrease a, constant V, $C_{s,0}$ and k_1. 5 – Constant a, V and $C_{s,0}$ decrease k_1.*

Results technology two – Nanopore technology and the detection cancer reporters

Template deposition produces particles with dimensions that are controlled by both the reaction time, and the template itself. Pores within the Al_2O_3 membranes had an average diameter of circa 300 nm, which determined the diameter of the growing particles. The length of the rod was controlled by the total charge passed (Figure 7). The composition of material within the rod can be controlled by varying the plating solution as well as the potential under which the reaction takes place.

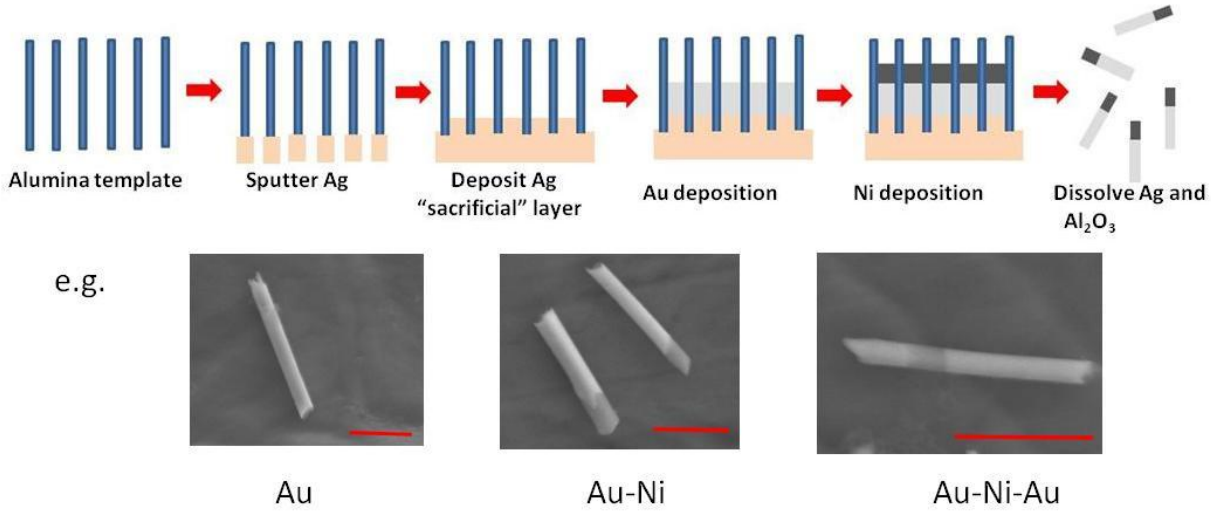

Figure 7*. Schematic of the particle synthesis. An alumina membrane is sputtered with a layer of Ag which acts as the electrode. First the pores are filled with a sacrificial silver layer, followed by layers of Au and Ni. The particles are released from the alumina by dissolution of the Ag and Al_2O_3. Examples of the composition of particles used in this study are shown below, Au rods (left) Au-Ni (middle) and Au-Ni-Au (right). Scale bar = 0.5μm.*

TP optimization.

Prior to performing an assay, Au rods of varying lengths (were synthesized to act as a set of control particles and aid the study of rod shaped particles as they traverse a TP. A unique property of TPs is the ability to stretch and relax the pore membrane, which can alter the inferred pore size by an order of magnitude . The membrane stretch is quantified by the increased separation of actuation points on a macroscopic pore specimen. A series of optimization experiments were performed to study the signal from cylindrical particles traversing the pores across a range of membrane stretches. This ensured that a pore size and potential figure 9 could be selected to produce a clear signal. The measurements (Figure 8) record Δi_p and FWHM as the membrane stretch is increased. Two sets of calibration spheres, 0.955 μm and 2 μm in diameter, and rods composed of Au, 2.1 μm and 4.7 μm in length were used.

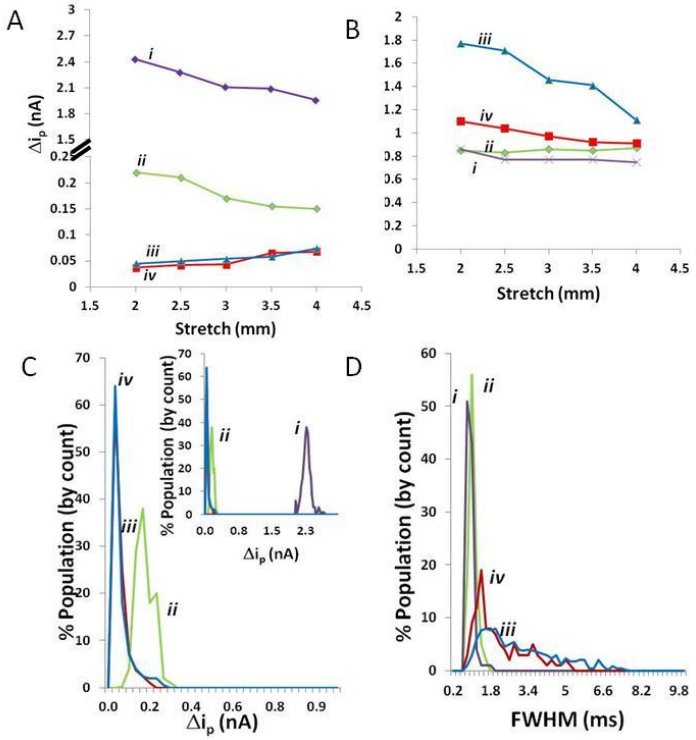

Figure 8. *Purple (i)= sphere (2 μm diameter), green(ii) = sphere (0.955 μm diameter), blue(iii) = Au rod (4.7 μm length-CV 14%, 290 nm diameter-CV 15%), red (iv)=Au rod (2.15 μm length-CV 20%, 325 nm diameter-CV 14%). A, Modal Δi_p values as pore size is varied, fixed potential of 0.12V. B, Modal FWHM values as pore size is varied, fixed potential of 0.12V. C, Δi_p histogram for the samples run at a stretch of 2.5 mm in part A. D, FWHM histogram for samples run at a stretch of 2.5 mm in part B.*

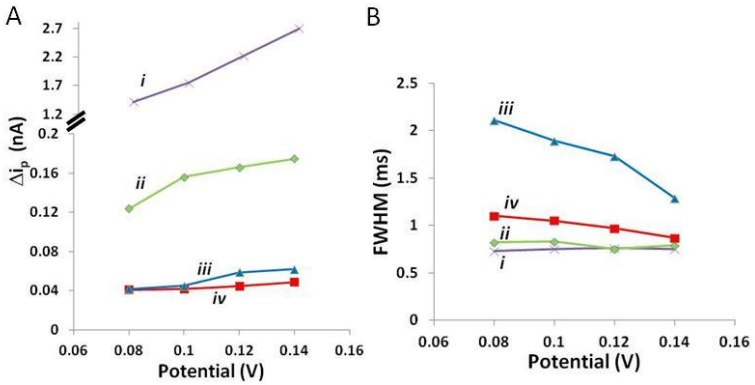

***Figure 9**. Purple (i)= sphere (2 μm diameter), green(ii) = sphere (0.955 μm diameter), blue(iii) = Au rod (4.7 μm length-CV 14%, 290 nm diameter-CV 15%), red (iv)=Au rod (2.15 μm length-CV 20%, 325 nm diameter-CV 14%). A, Modal Δi_p as potential is varied, fixed stretch of 2.5 mm. B, Modal FWHM values as potential is varied, fixed stretch of 2.5 mm.*

In Figure 8A, Δi_p decreases for the spherical particles as the membrane stretch is increased, matching previous observations for similar systems, and is consistent with Equation 1. In contrast, Δi_p appears to be constant or slightly increasing for the rods. As the pore size increases, the rods are more likely to be tilted with respect to the pore axis. Tilted rods will displace a greater volume of electrolyte near the pore constriction when the peak current change is measured, producing an increase in pulse size.

Simulated Δi_p and FWHM

Simulated resistive pulses in Figure 10 were carried out using a semi-analytic model.

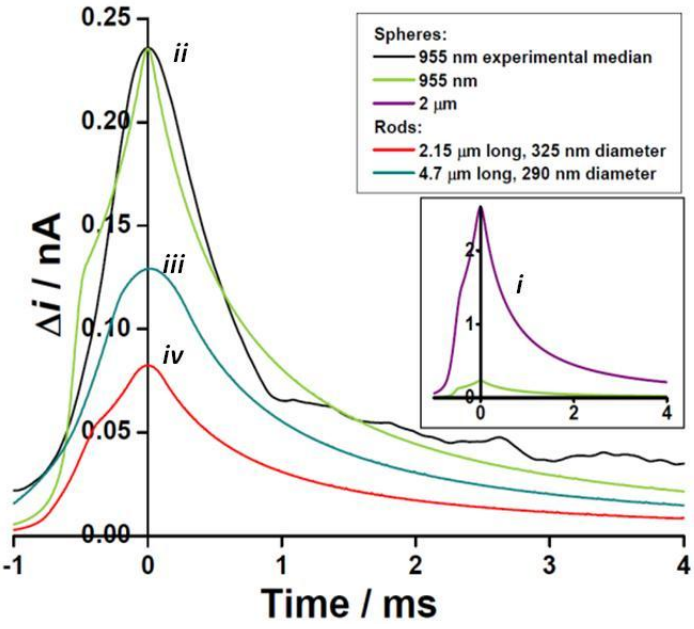

***Figure 10.** Simulated resistive pulses corresponding to the particles studied in Figure 3, purple (i)= sphere (2 μm diameter), green(ii) = sphere (0.955 μm diameter), blue(iii) = Au rod (4.7 μm length, 290 nm diameter), red (iv)=Au rod (2.15 μm length, 325 nm diameter). Ccalibrated using data for 955 nm spheres at X = 2.5 mm and 0.12 V. Inset: An expanded vertical axis allows comparison with the simulation for a 2 μm sphere.*

Briefly, the model assumes conical pore geometry with a symmetric constriction close to the membrane surface containing the smaller pore opening (Figure 2A). Simulations were calibrated using the experiment for 955 nm spheres at 2.5 mm stretch and 0.12 V, by matching the baseline current, as well as typical pulse magnitude, duration, and asymmetry. The resulting fitted parameters were 168.5 Pa across the membrane, with pore opening radii 14.6 and 2.1 μm, and a constriction 4.1 μm below the pore surface. Simulated resistive pulses assume that the rods are not tilted.

Figure 10 shows that although Δi_p is predicted to vary by more than an order of magnitude between the four particle sets, the predicted response closely follows the experimental values (Figure 8). Predicted and measured Δi_p and FWHM values at 2.5 mm stretch and 0.12V are listed in Table 1. The largest deviation from simulated values occurs for the FWHM of the longer 4.7 μm rods. It is clear from Figure 8B that across all stretches the two rod shaped particles produce a FWHM value

larger than the spherical beads, with 4.7 μm long rods recording the largest FWHM values, which implies the longest translocation time.

Demonstration assay.

A control experiment was performed to determine the sensitivity of the TP to solutions containing mixtures of the 2.1 μm and 4.7 μm Au rods, Figure 5. Initially a solution containing only 2.1 μm rods was analyzed. The mole fraction of the 4.7 μm rod was then increased. Modal Δi_p (Figure 11A) and FWHM (Figure 11B) values are plotted as a percentage change from the initial value for 2.1 μm rods. The measured values for Δi_p matched the simulated results reasonably well (dashed lines). FWHM values increase with the increasing fraction of 4.7 mm rods, and whilst the simulated results match this trend, they significantly underestimate the experimental values.

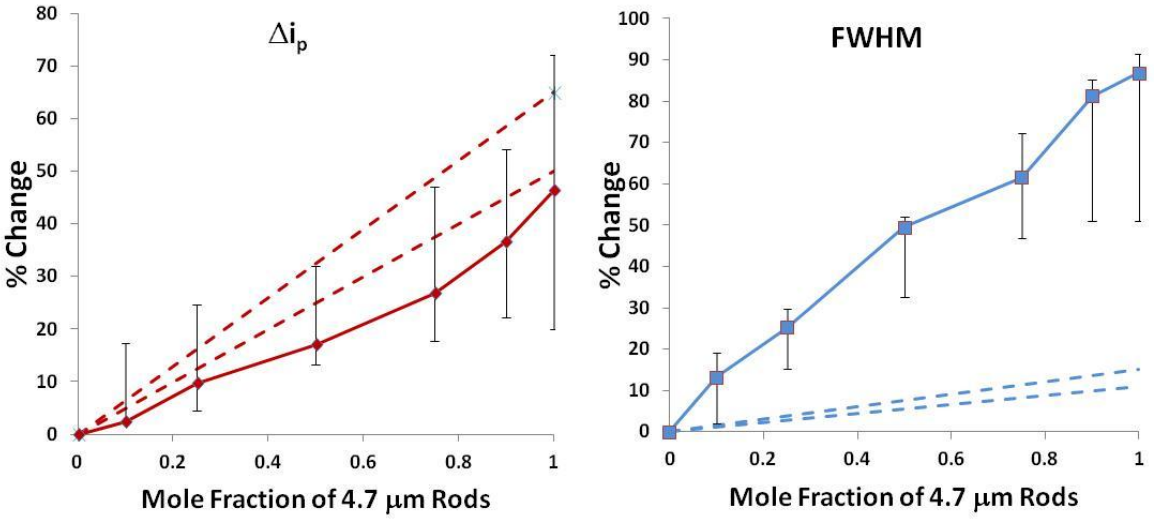

Figure 11. *Changes in Δi_p and FWHM as mole fraction of 4.7 μm rods is increased. Dashed lines join the maximum and minimum values predicted by simulations for 0% and 100% molar fraction, given the CV of 4.7 μm rod size distribution. Error bars show the d25 and d75 values for each data point, lines joining data points are drawn to guide the eye.*

	Δi_p (nA)		FWHM (ms)	
	Simulated	Measured	Simulated	Measured
2 μm Sphere	0.24	0.21	1.06	0.83
0.955 μm Sphere	2.59	2.28	1.01	0.77
2.1 μm Rod	0.08	0.05	1.13	0.91
4.17 μm Rod	0.13	0.06	1.30	1.90

Table 1*. Modal experimental measurements and simulated values for Δi_p and FWHM, using a potential of 0.12 V and a stretch of 2.5 mm.*

Agglutination assay

Avidin-biotin assay.

Using rod shaped particles for an agglutination assay could result in the particles coming together in number of different configurations, resulting in trends within FWHM and Δi_p which are difficult to interpret. One solution is to control the orientation of aggregation. In the experiments outlined below, Ni was incorporated into the rods, either at the end of the rod or as a segment in the middle. This was done for two reasons, firstly to make handing the rods much easier during any surface chemistry modifications and subsequent wash stages, as the rods could be separated from solution

using a simple hand held magnet as opposed to centrifugation. Secondly, the Ni surface could act as a locus for the capture probe, producing a "sticky" Ni segment that captures the analyte and acts as the centre for aggregation.

A schematic of the agglutination assays are shown in Figure 12. Capture probes were conjugated to the Ni surface using first a His-modified peptide, followed by EDC or SMCC chemistry, described below. Two different capture probes were conjugated to the rods, the first example used the avidin protein. To confirm the surface chemistry performed as shown in the schematic, the Ni modified avidin particles were incubated for 5 minutes with a solution of biotinylated-FITC. A localized fluorescent signal on the Ni, confirmed its success, Figure 12B. The particles have a residual net magnetization in the absence of an applied field; a consequence of this was slow aggregation of the particles if they were left in solution without sonication for periods longer than 30 minutes.

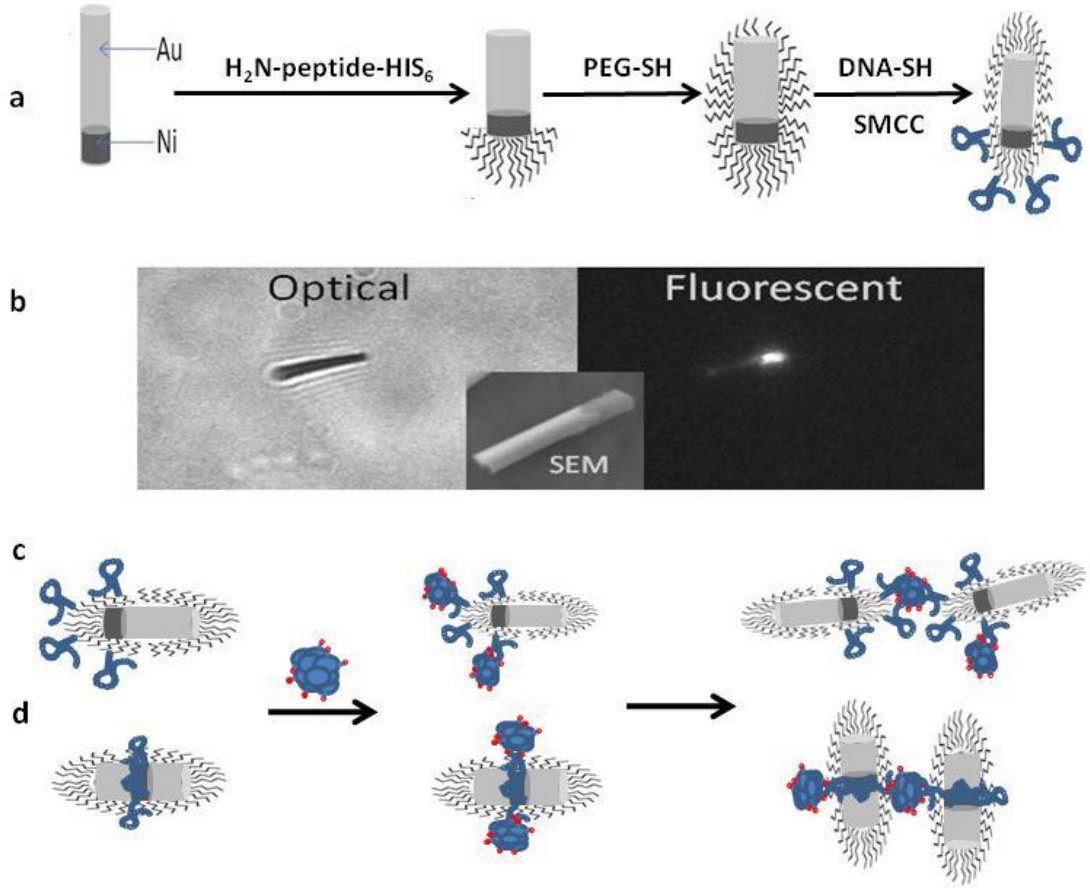

Figure 12*. Overview of the surface chemistry modifications and assays. a - The surfaces of the Ni segments are modified with a His-tagged peptide, the Au segments are modified with PEG-SH molecules. b – Confirmation of localised surface chemistries with fluorescent modified Ni segments. c – Schematic of the aggregation assay via "end-on-end" aggregation. d – Schematic of the aggregation assay via "side-on" aggregation.*

By controlling the orientation of the rods' interaction, rods of similar aspect ratios could be used to identify the presence of a target analyte, thus making agglutination assays easier to multiplex with TPs. If the rods aggregated end-on-end (Figure 12C) there was a simultaneous increase in Δi_p and FWHM, as opposed to rods aggregating in a side-on configuration (Figure 12D), where only a change in Δi_p was observed. Figure 13A shows the percentage change in Δi_p and FWHM for 1 μm rods, end functionalized with Ni, in a buffered solution. The solution was placed on a rotating wheel and sampled at 5 min intervals. A slight increase in Δi_p and FWHM was measured over 15 minutes. The result indicates that the Ni caused some nonspecific aggregation, however it occurs at a level low enough to not be the dominant signal during the aggregation in the presence of an analyte. The

calculated mutual diffusion coefficient for the rod was 5.6×10^{-8} cm^2s^{-1}, for a length and radius of 1 μm and 150 nm. An assay time of 10 min was chosen, using a concentration of particles circa 300-500 fM, as these conditions should allow sufficient time for the assay to be completed, given that the rate determining step is the diffusion of the analyte to the rods. The rods were sonicated and an aliquot was drawn from the stock solution, an equal volume of analyte solution was then added, concentrations of analyte in the inital solution are plotted on all graphs. At the start of each assay a blank was measured after 10 minutes, to allow the percentage change for FWHM and Δi_p to be calculated in subsequent samples. Figure 13B shows the percentage change in Δi_p and FWHM for an assay using end functionalized rods, where the Ni segment has been conjugated to avidin and the target protein was a biotinylated-BSA, which contained on average 9 biotins/ protein. The same rod sample was incubated with a non-biotinylated protein solution, and the resulting changes in Δi_p and FWHM are shown as dashed lines in Figure 13B. The absence of signal change for the non biotinyated target demonstrates that the rods are not non-specifically aggregating around the protein. A similar protocol was used for the rods containing a Ni segment in the middle of the rod, with results shown in Figure 13C.

2.2.2 PDGF assay.

We finally demonstrated the end-on-end assay format again for the detection of PDGF. It is known that the aptamer binds to the protein in a 2:1 ratio and has previously been used in an agglutination assay using gold particles and a colorimetric detection mechanism. As with the avidin example above, we observed an increase in both the Δi_p and FWHM (Figure 13D). A control assay for the same rods using a different protein (BSA) produced small changes in FWHM and $\Delta i_{p,}$ (Figure 13D circled data points), demonstrating that the aggregation was not nonspecific.

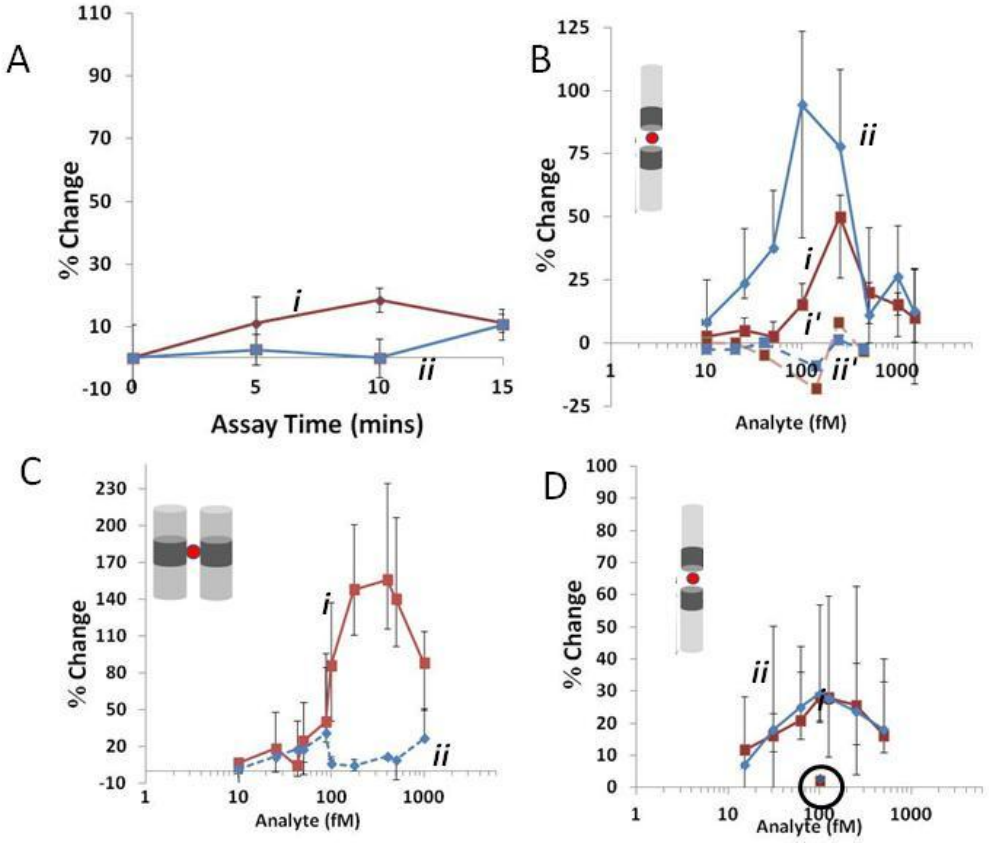

Figure 13. *Agglutination assay data collected at stretch=2.5mm, potential =0.14, where red (i) indicate Δi_p and blue (ii) indicate FWHM. A,variation in Δi_p and FWHM for 400fM AuNi rods (1.23 μm long with CV 20%, Ni content 15% by length) as assay time is increased in the absence of an analyte. B, the same rods as A at assay time 10 mins. Ni segments*

are functionalised with avidin and the concentration of the biotinylated-BSA analyte is varied. Dashed lines represent a 10 min assay with a non biotinylated target. C, a biotin-avidin assay at 10 mins as in B, using 500 fM AuNiAu rods (0.82 μm long with CV 14%, Ni content 18% by length) in the side-on configuration. D, 150fM AuNi rods (1.1 μm long with CV 20%, Ni content 14% by length) at assay time 10 mins. Ni segments are functionalised with PDGF aptamer, and the analyte is PDGF. The circled data points at 100 fM indicate the change in FWHM and Δi_p for the same rods using a control protein. Error bars show the d25 and d75, values for each data point, lines joining data points are drawn to guide the eye.

Discussion

Rod Orientation

End-on, axially symmetric rod orientation is a natural starting point for analysing and simulating rod resistive pulses events. Particle transport is dominated by pressure-driven flow, which is focused at the centre of the pore, encouraging alignment of the rods on-axis. This flow has been observed previously to produce a shear force capable of causing weakly interacting particles to dissociate at the pore mouth. Notwithstanding, if a pore can allow a 2 μm sphere to pass through, is would imply that a 2.1 μm rod could traverse the pore in any orientation.

Experimental FWHM values for rods are much larger than the modeled values. The most likely explanation for this is that rods do deviate from end-on orientation and can interact with each other and the pore walls, slowing the particles as they traverse the opening. Increased dwell time can also be explained by slower hydrodynamic motion of off-axis or tilted particles. This interpretation is supported by the long 'tail' of slow-moving particles evident for rods in the duration histogram, Figure 8D, which is responsible for the large differences in FWHM observed with the demonstration assay (Figure 11B). The orientation effect seems to be exaggerated as the length of the rod is increased, and the largest deviation from measured to modeled values appears at the FWHM for larger 4.7 μm rods. This interpretation is consistent with the hypothesis that, for rods, Δi_p increases at larger pore stretches due to a change in rod orientation. A skewed distribution is also evident for rods in the Δi_p histogram, Figure 8C

Regardless of whether the quantitative FWHM duration can be accurately predicted, this measurement provides a clear basis for distinguishing rod-like particles: despite the 2.1 μm rods possessing a dimension similar to the 2 μm diameter sphere, the rod particles produce a significantly larger FWHM, Figure 8B. As the rod length is increased, the FWHM values also clearly increase.

Agglutination assay

In the end-to-end avidin-biotin assay, increased concentration of the analyte caused two trends in the recorded values (Figure 13B). Firstly, both the Δi_p and FWHM values increase, and continued up to a concentration ~ 250 fM, before the binding sites on the Ni segments become saturated, and a hook effect is observed. Secondly, and more importantly, the FWHM is the dominant signal as the rods aggregate, forming longer particles. The increase in rod length, as demonstrated within the control assay, Figure 11B, resulted in FWHM changes that were proportionally larger than those for Δi_p. Results from the side-on assay in Figure 13C show that, while an increase in analyte concentration caused a clear increase in Δi_p, the FWHM did not change significantly. The side-on orientation forms rod aggregates with increased diameters but constant length. Trends for the end-on-end PDGF assay (Figure 13D) were similar to those for the end-on-end biotin assay. However the percentage change in both the FWHM and Δi_p was much lower than for avidin–biotin, indicating that fewer aggregates were formed in the PDGF assay.

Improving assay sensitivity

The K_d for the PDGF aptamer and its target is four orders of magnitude higher than that of the avidin and biotin system. Therefore the smaller percentage changes in signal for the PDGF system is attributed to slower rates of reaction between the rod and protein, which has been shown to be the rate limiting step in the formation of aggregates. The limits of detection here is as low as 10 fM, 5 orders of magnitude lower than colorimetric assays using the same capture probe. Once the analyte is captured onto a rod, residual magnetization of the Ni facilitates the formation of aggregates as the

probability of two particles colliding and resulting in an aggregate is enhanced. This effect is shown in Figure 13A, illustrating that particles over time form non-specific aggregates through the magnetic interactions. The residual magnetization also has the effect of reducing the rate at which the particles separate. The force holding the particles together (F_A) is the sum of the force from the biological interaction (F_b) plus the magnetic interaction force, F_m (calculated here to be 0.4pN).

$$F_A = F_b + F_m \quad (2)$$

The sum of these two forces holds the particles together once a successful collision event has occurred, improving the sensitivity by prolonging the aggregate lifetime. This observation could help design agglutination assays for use in TPs. Rod shaped particles may also have an advantage over spherical particles as they possess a planar surface to which the capture probe is anchored. This has recently been shown to enhance the association rates for triangular particles in DNA conjugation studies[63]. The last factor which aids sensitivity is the measurement technique. Unlike detection formats such as light scattering or colorimetric assays, where the physical properties of the entire population of particles are measured simultaneously, with RPS each particle is measured independently as they traverse the pore. While this technique has a lower throughput than ensemble methods (circa 1000 particles a minute), it is potentially more accurate because the measurement is not dominated by outliers in the particle distribution. A major benefit of TPs for aggregation assays is that the user can remove any blockages that may occur during the assay by stretching the membrane, allowing larger aggregates to pass through the channel. Once the blockage has been removed the pore size can be returned back to its original size and the data collection continued.

The movement of rod shaped particles through TPs has been studied. It was demonstrated that as the rods traverse the pores, the resistive pulse magnitude is sensitive to the size of the particle, whereas the FWHM values give a clear indication of the length. Recorded FWHM durations increase with the length of the rod, and are much longer than predicted in simulations. This can be explained by variation in the orientation of rods passing through TPs, resulting in steric interactions which slow the particles. Variations of rod orientation offer an intriguing additional parameter for monitoring particle behaviour. An agglutination assay was designed in which the orientation of rods coming together was controlled, so that either the resistive pulse magnitude or duration could be used as the indicator for analyte detection. The assay was demonstrated using multicomponent rods composed of Ni and Au. The Ni segment can be selectively activated with a capture probe of interest, and act as a locus for aggregation. The control of the dominant signal created when rods aggregate could make agglutination assays much easier to multiplex, as similar sized rods can be used for two different targets, simplifying particle synthesis. The sensitivity of the assay is aided by the multicomponent rods and the residual magnetisation, and is comparable to that of ELISA. The simple and fast format described here could be of benefit for point of care technologies.

Potential impact or the research

The impact of these results is the identification of key parameters for agglutination assay shown in figure 6. These results provide a foundation unto which the future development of assays can be built upon. They have proved a suitable starting point for the development for the rod assay. By using asymmetric particles such as rods we further enhance the scope of the agglutination assay by demonstrating that similar aspect ratio particles can be made to produce two distant signal sets by controlling their orientation. This has lead to a patent application being submitted using the controlled aggregation of nanorods for the detection of analytes.

The results in conjunction with the patent application have lead to commercial interest from Izon, a company that produces nanopore devices. The research above have been presented at two international conferences, via both oral and poster presentations increasing the profile of the fellow and the Marie Curie funding scheme.

4.1 se and dissemination of foreground

A plan for use and dissemination of foreground (including socio-economic impact and target groups for the results of the research) shall be established at the end of the project. It should, where appropriate, be an update of the initial plan in Annex I for use and dissemination of foreground and be consistent with the report on societal implications on the use and dissemination of foreground (section 4.3 – H).

The plan should consist of:

- Section A

  This section should describe the dissemination measures, including any scientific publications relating to foreground. **Its content will be made available in the public domain** thus demonstrating the added-value and positive impact of the project on the European Union.

- Section B

  This section should specify the exploitable foreground and provide the plans for exploitation. All these data can be public or confidential; the report must clearly mark non-publishable (confidential) parts that will be treated as such by the Commission. Information under Section B that is not marked as confidential **will be made available in the public domain** thus demonstrating the added-value and positive impact of the project on the European Union.

Section A (public)

This section includes two templates

- Template A1: List of all scientific (peer reviewed) publications relating to the foreground of the project.
- Template A2: List of all dissemination activities (publications, conferences, workshops, web sites/applications, press releases, flyers, articles published in the popular press, videos, media briefings, presentations, exhibitions, thesis, interviews, films, TV clips, posters).

These tables are cumulative, which means that they should always show all publications and activities from the beginning until after the end of the project. Updates are possible at any time.

TEMPLATE A1: LIST OF SCIENTIFIC (PEER REVIEWED) PUBLICATIONS, STARTING WITH THE MOST IMPORTANT ONES

NO.	Title	Main author	Title of the periodical or the series	Number, date or frequency	Publisher	Place of publication	Year of publication	Relevant pages	Permanent identifiers[1] (if available)	Is/Will open access[2] provided to this publication?
1	Detection of biotin and herpes simplex virus 1 and 2 with a magnetic bead aggregation (MBA) assay	*Mark Platt*	*Analytical chemistry*	*Feb 2012*	*ACS*	*USA*	*2012*			yes
2	M13Bacteriaphage-Activated Superparamagnetic Beads for Affinity Separation	Julien Muzzard	Small	In press	Wiley	EU	2012			yes
3		Mark	Small	In press	Wiley	EU	2012			yes

[1] A permanent identifier should be a persistent link to the published version full text if open access or abstract if article is pay per view) or to the final manuscript accepted for publication (link to article in repository).

[2] Open Access is defined as free of charge access for anyone via Internet. Please answer "yes" if the open access to the publication is already established and also if the embargo period for open access is not yet over but you intend to establish open access afterwards.

	Resistive pulse sensing of analyte-induced multicomponent rod aggregation using tunable pores	Platt								
4	Resistive pulse sensing of magnetic beads and supraparticle structures using tunable pores	Geoff Willmott	Biomicrofluidics	Dec 2011	AIP	USA	2011			yes
5	*Self-Assembly of Superparamagnetic Microparticles with high surface area: controlling morphology through drying conditions*	James O Mahony	In preparation							
6	Separation of superparamagnetic beads using FNLM	Peng Li	Article in preparation							

TEMPLATE A2: LIST OF DISSEMINATION ACTIVITIES

NO.	Type of activities[3]	Main leader	Title	Date	Place	Type of audience[4]	Size of audience	Countries addressed
1	Conference		Analysis for Healthcare Diagnostics and Theranostics	06 September 2010 to 08 September 2010	Edinburgh	Scientific	200	
2	Conference		Electrochem	05 September	Bath	Scientific	50	

[3] A drop down list allows choosing the dissemination activity: publications, conferences, workshops, web, press releases, flyers, articles published in the popular press, videos, media briefings, presentations, exhibitions, thesis, interviews, films, TV clips, posters, Other.

[4] A drop down list allows choosing the type of public: Scientific Community (higher education, Research), Industry, Civil Society, Policy makers, Medias ('multiple choices' is possible.

			2011	2011 09:00 - 06 September 2011				
3	Conference		Smart surfaces 2012	6th March – 9th March 2012	Dublin	Scientific		

Section B (Confidential[5] or public: confidential information to be marked clearly)
Part B1

The applications for patents, trademarks, registered designs, etc. shall be listed according to the template B1 provided hereafter.

The list should, specify at least one unique identifier e.g. European Patent application reference. For patent applications, only if applicable, contributions to standards should be specified. This table is cumulative, which means that it should always show all applications from the beginning until after the end of the project.

TEMPLATE B1: LIST OF APPLICATIONS FOR PATENTS, TRADEMARKS, REGISTERED DESIGNS, ETC.					
Type of IP Rights[6]:	Confidential Click on YES/NO	Foreseen embargo date dd/mm/yyyy	Application reference(s) (e.g. EP123456)	Subject or title of application	Applicant (s) (as on the application)
Patent application	yes		U02-759-02GB	*Detection of biomarkers using nanopore and nanorod technology*	Mark Platt, Gil U lee
patent	yes		PCT/EP2011/061550.	*Non-linear magnetophoretic separation device, system and method. Patent application*	P. Li, M. Platt, G. Cannon, G. U. Lee

[5] Note to be confused with the "EU CONFIDENTIAL" classification for some security research projects.

[6] A drop down list allows choosing the type of IP rights: Patents, Trademarks, Registered designs, Utility models, Others.

Part B2
Please complete the table hereafter:

Type of Exploitable Foreground[7]	Description of exploitable foreground	Confidential Click on YES/NO	Foreseen embargo date dd/mm/yyyy	Exploitable product(s) or measure(s)	Sector(s) of application[8]	Timetable, commercial or any other use	Patents or other IPR exploitation (licences)	Owner & Other Beneficiary(s) involved
	Ex: New supercond uctive Nb-Ti alloy			*MRI equipment*	*1. Medical 2. Industrial inspection*	*2008 2010*	*A materials patent is planned for 2006*	*Beneficiary X (owner) Beneficiary Y, Beneficiary Z, Poss. licensing to equipment manuf. ABC*

In addition to the table, please provide a text to explain the exploitable foreground, in particular:

- Its purpose
- How the foreground might be exploited, when and by whom
- IPR exploitable measures taken or intended
- Further research necessary, if any
- Potential/expected impact (quantify where possible)

[19] A drop down list allows choosing the type of foreground: General advancement of knowledge, Commercial exploitation of R&D results, Exploitation of R&D results via standards, exploitation of results through EU policies, exploitation of results through (social) innovation.
[8] A drop down list allows choosing the type sector (NACE nomenclature) : http://ec.europa.eu/competition/mergers/cases/index/nace_all.html

4.2 Report on societal implications

Replies to the following questions will assist the Commission to obtain statistics and indicators on societal and socio-economic issues addressed by projects. The questions are arranged in a number of key themes. As well as producing certain statistics, the replies will also help identify those projects that have shown a real engagement with wider societal issues, and thereby identify interesting approaches to these issues and best practices. The replies for individual projects will not be made public.

A General Information *(completed automatically when **Grant Agreement number** is entered.*	
Grant Agreement Number:	252935
Title of Project:	Magnetic Nanoparticles for multiplexed assays for low and high molecular weight biomarkers.
Name and Title of Coordinator:	Prof Gil U. Lee

B Ethics	
1. Did your project undergo an Ethics Review (and/or Screening)? • If Yes: have you described the progress of compliance with the relevant Ethics Review/Screening Requirements in the frame of the periodic/final project reports? Special Reminder: the progress of compliance with the Ethics Review/Screening Requirements should be described in the Period/Final Project Reports under the Section 3.2.2 *'Work Progress and Achievements'*	***NO***
2. Please indicate whether your project involved any of the following issues (tick box) :	***YES***
RESEARCH ON HUMANS	
• Did the project involve children?	
• Did the project involve patients?	
• Did the project involve persons not able to give consent?	
• Did the project involve adult healthy volunteers?	
• Did the project involve Human genetic material?	
• Did the project involve Human biological samples?	
• Did the project involve Human data collection?	
RESEARCH ON HUMAN EMBRYO/FOETUS	
• Did the project involve Human Embryos?	
• Did the project involve Human Foetal Tissue / Cells?	
• Did the project involve Human Embryonic Stem Cells (hESCs)?	
• Did the project on human Embryonic Stem Cells involve cells in culture?	
• Did the project on human Embryonic Stem Cells involve the derivation of cells from Embryos?	
PRIVACY	
• Did the project involve processing of genetic information or personal data (eg. health, sexual lifestyle, ethnicity, political opinion, religious or philosophical conviction)?	
• Did the project involve tracking the location or observation of people?	
RESEARCH ON ANIMALS	
• Did the project involve research on animals?	
• Were those animals transgenic small laboratory animals?	
• Were those animals transgenic farm animals?	

• Were those animals cloned farm animals?	
• Were those animals non-human primates?	
RESEARCH INVOLVING DEVELOPING COUNTRIES	
• Did the project involve the use of local resources (genetic, animal, plant etc)?	
• Was the project of benefit to local community (capacity building, access to healthcare, education etc)?	
DUAL USE	
• Research having direct military use	0 Yes 0 No
• Research having the potential for terrorist abuse	

C Workforce Statistics

3. Workforce statistics for the project: Please indicate in the table below the number of people who worked on the project (on a headcount basis).

Type of Position	Number of Women	Number of Men
Scientific Coordinator		1
Work package leaders		1
Experienced researchers (i.e. PhD holders)		1
PhD Students		
Other		

4. How many additional researchers (in companies and universities) were recruited specifically for this project?	
Of which, indicate the number of men:	0

D Gender Aspects

5. Did you carry out specific Gender Equality Actions under the project?	○ x	Yes No

6. Which of the following actions did you carry out and how effective were they?

	Not at all effective				Very effective
❑ Design and implement an equal opportunity policy	○	○	○	○	○
❑ Set targets to achieve a gender balance in the workforce	○	○	○	○	○
❑ Organise conferences and workshops on gender	○	○	○	○	○
❑ Actions to improve work-life balance	○	○	○	○	○

○ Other:

7. Was there a gender dimension associated with the research content – i.e. wherever people were the focus of the research as, for example, consumers, users, patients or in trials, was the issue of gender considered and addressed?

○ Yes- please specify

○ No

E Synergies with Science Education

8. Did your project involve working with students and/or school pupils (e.g. open days, participation in science festivals and events, prizes/competitions or joint projects)?

x Yes- please specify

○ No

9. Did the project generate any science education material (e.g. kits, websites, explanatory booklets, DVDs)?

○ Yes- please specify

○ No

F Interdisciplinarity

10. Which disciplines (see list below) are involved in your project?

○ Main discipline[9]:

○ Associated discipline[9]: ○ Associated discipline[9]:

G Engaging with Civil society and policy makers

11a Did your project engage with societal actors beyond the research community? *(if 'No', go to Question 14)*	○ ○	Yes No

11b If yes, did you engage with citizens (citizens' panels / juries) or organised civil society (NGOs, patients' groups etc.)?

○ No

○ Yes- in determining what research should be performed

○ Yes - in implementing the research

○ Yes, in communicating /disseminating / using the results of the project

[9] Insert number from list below (Frascati Manual).

11c In doing so, did your project involve actors whose role is mainly to organise the dialogue with citizens and organised civil society (e.g. professional mediator; communication company, science museums)?	○ ○	Yes No

12. Did you engage with government / public bodies or policy makers (including international organisations)

- ○ No
- ○ Yes- in framing the research agenda
- ○ Yes - in implementing the research agenda
- ○ Yes, in communicating /disseminating / using the results of the project

13a Will the project generate outputs (expertise or scientific advice) which could be used by policy makers?

- ○ Yes – as a **primary** objective (please indicate areas below- multiple answers possible)
- ○ Yes – as a **secondary** objective (please indicate areas below - multiple answer possible)
- ○ No

13b If Yes, in which fields?

Agriculture		Energy		Human rights	
Audiovisual and Media		Enlargement		Information Society	
Budget		Enterprise		Institutional affairs	
Competition		Environment		Internal Market	
Consumers		External Relations		Justice, freedom and security	
Culture		External Trade		Public Health	
Customs		Fisheries and Maritime Affairs		Regional Policy	
Development Economic and Monetary Affairs		Food Safety		Research and Innovation	
		Foreign and Security Policy		Space	
Education, Training, Youth		Fraud		Taxation	
Employment and Social Affairs		Humanitarian aid		Transport	

13c If Yes, at which level?

- ○ Local / regional levels
- ○ National level
- ○ European level
- ○ International level

H Use and dissemination

14. How many Articles were published/accepted for publication in peer-reviewed journals?	**6**
To how many of these is open access[10] provided?	**6**
How many of these are published in open access journals?	**6**
How many of these are published in open repositories?	
To how many of these is open access not provided?	
Please check all applicable reasons for not providing open access:	
❑ publisher's licensing agreement would not permit publishing in a repository ❑ no suitable repository available ❑ no suitable open access journal available ❑ no funds available to publish in an open access journal ❑ lack of time and resources ❑ lack of information on open access ❑ other[11]: ……	

15. How many new patent applications ('priority filings') have been made? *("Technologically unique": multiple applications for the same invention in different jurisdictions should be counted as just one application of grant).*		**3**
16. Indicate how many of the following Intellectual Property Rights were applied for (give number in each box).	Trademark	
	Registered design	
	Other	
17. How many spin-off companies were created / are planned as a direct result of the project?		**0**
Indicate the approximate number of additional jobs in these companies:		

18. Please indicate whether your project has a potential impact on employment, in comparison with the situation before your project:

x	Increase in employment, or	❑	In small & medium-sized enterprises
❑	Safeguard employment, or	❑	In large companies
❑	Decrease in employment,	❑	None of the above / not relevant to the project
❑	Difficult to estimate / not possible to quantify		

19. For your project partnership please estimate the employment effect resulting directly from your participation in Full Time Equivalent (*FTE = one person working fulltime for a year*) jobs:	*Indicate figure:*

[10] Open Access is defined as free of charge access for anyone via Internet.
[11] For instance: classification for security project.

Difficult to estimate / not possible to quantify	❑

I Media and Communication to the general public

20. As part of the project, were any of the beneficiaries professionals in communication or media relations?

○ Yes ○ No

21. As part of the project, have any beneficiaries received professional media / communication training / advice to improve communication with the general public?

○ Yes ○ No

22 Which of the following have been used to communicate information about your project to the general public, or have resulted from your project?

❑	Press Release	❑	Coverage in specialist press
❑	Media briefing	❑	Coverage in general (non-specialist) press
❑	TV coverage / report	❑	Coverage in national press
❑	Radio coverage / report	❑	Coverage in international press
❑	Brochures /posters / flyers	❑	Website for the general public / internet
❑	DVD /Film /Multimedia	❑	Event targeting general public (festival, conference, exhibition, science café)

23 In which languages are the information products for the general public produced?

❑	Language of the coordinator	❑	English
❑	Other language(s)		

***Question F-10*:** Classification of Scientific Disciplines according to the Frascati Manual 2002 (Proposed Standard Practice for Surveys on Research and Experimental Development, OECD 2002):

FIELDS OF SCIENCE AND TECHNOLOGY

1. NATURAL SCIENCES

1.1 Mathematics and computer sciences [mathematics and other allied fields: computer sciences and other allied subjects (software development only; hardware development should be classified in the engineering fields)]

1.2 Physical sciences (astronomy and space sciences, physics and other allied subjects)

1.3 Chemical sciences (chemistry, other allied subjects)

1.4 Earth and related environmental sciences (geology, geophysics, mineralogy, physical geography and other geosciences, meteorology and other atmospheric sciences including climatic research, oceanography, vulcanology, palaeoecology, other allied sciences)

1.5 Biological sciences (biology, botany, bacteriology, microbiology, zoology, entomology, genetics, biochemistry, biophysics, other allied sciences, excluding clinical and veterinary sciences)

2 ENGINEERING AND TECHNOLOGY

2.1 Civil engineering (architecture engineering, building science and engineering, construction engineering, municipal and structural engineering and other allied subjects)

2.2 Electrical engineering, electronics [electrical engineering, electronics, communication engineering and systems, computer engineering (hardware only) and other allied subjects]

2.3. Other engineering sciences (such as chemical, aeronautical and space, mechanical, metallurgical and materials engineering, and their specialised subdivisions; forest products; applied sciences such as

geodesy, industrial chemistry, etc.; the science and technology of food production; specialised technologies of interdisciplinary fields, e.g. systems analysis, metallurgy, mining, textile technology and other applied subjects)

3. MEDICAL SCIENCES

3.1 Basic medicine (anatomy, cytology, physiology, genetics, pharmacy, pharmacology, toxicology, immunology and immunohaematology, clinical chemistry, clinical microbiology, pathology)

3.2 Clinical medicine (anaesthesiology, paediatrics, obstetrics and gynaecology, internal medicine, surgery, dentistry, neurology, psychiatry, radiology, therapeutics, otorhinolaryngology, ophthalmology)

3.3 Health sciences (public health services, social medicine, hygiene, nursing, epidemiology)

4. AGRICULTURAL SCIENCES

4.1 Agriculture, forestry, fisheries and allied sciences (agronomy, animal husbandry, fisheries, forestry, horticulture, other allied subjects)

4.2 Veterinary medicine

5. SOCIAL SCIENCES

5.1 Psychology

5.2 Economics

5.3 Educational sciences (education and training and other allied subjects)

5.4 Other social sciences [anthropology (social and cultural) and ethnology, demography, geography (human, economic and social), town and country planning, management, law, linguistics, political sciences, sociology, organisation and methods, miscellaneous social sciences and interdisciplinary , methodological and historical S1T activities relating to subjects in this group. Physical anthropology, physical geography and psychophysiology should normally be classified with the natural sciences].

6. HUMANITIES

6.1 History (history, prehistory and history, together with auxiliary historical disciplines such as archaeology, numismatics, palaeography, genealogy, etc.)

6.2 Languages and literature (ancient and modern)

6.3 Other humanities [philosophy (including the history of science and technology) arts, history of art, art criticism, painting, sculpture, musicology, dramatic art excluding artistic "research" of any kind, religion, theology, other fields and subjects pertaining to the humanities, methodological, historical and other S1T activities relating to the subjects in this group]